Available online at http://scik.org
J. Math. Comput. Sci. 6 (2016), No. 1, 39-57
ISSN: 1927-5307

A REVIEW OF IMAGE RECONSTRUCTION METHODS IN ELECTRICAL CAPACITANCE TOMOGRAPHY

JOSIAH NOMBO[1,2,*], ALFRED MWAMBELA[2], MICHAEL KISANGIRI[1]

[1]Department of Communication Science and Engineering,
Nelson Mandela African Institution of Science and Technology, Arusha, Tanzania
[2]Department of Electronics and Telecommunication Engineering,
University of Dar es Salaam, Dar es Salaam, Tanzania

Abstract. In this paper, we review image reconstruction methods and their suitability in electrical capacitance tomography measurement system. These methods can be grouped into direct and iterative methods. Direct methods include Linear back projection, Singular value decomposition, and Tikhonov regularization. Iterative methods are further divided into algebraic and optimization methods. Algebraic reconstruction methods include iterative linear back projection, iterative Tikhonov, Landweber iteration, simultaneously algebraic reconstruction, and model−based reconstruction. Optimization methods include fuzzy mathematical modeling, genetic algorithms, artificial neural networks, generalized vector sampled pattern matching, total variation regularization, regularized total least squares, extended Tikhonov regularization, simulated annealing, compressed sensing principle, population entropy, adaptive differential evolution, least−squares support vector machine, and self-adaptive particle swarm optimization. Some of these methods have been examined through experiments and their comparative analysis have been given. Results show that iterative methods generate high quality images compared with non-iterative ones when evaluated over full component fraction range. However, iterative methods are computationally expensive, and hence used for research and off-line investigations rather than for on-line process monitoring.

Keywords: Electrical capacitance tomography; Inverse problem; Image reconstruction.

2010 AMS Subject Classification: 65K05, 65K10.

*Corresponding author

Received August 13, 2015

1. Introduction

Tomography is a non-destructive imaging technique that creates an image of an object's internal structure. The technique has been used in radiology, archeology, biology, atmospheric, geophysics, oceanography, plasma physics, materials science, astrophysics, quantum information, and other sciences [2, 12, 26].

Tomography imaging can be divided into two types: hard-field and soft-field tomography [9, 27]. In hard-field tomography, the direction of travel of energy waves from the power source is constant regardless of the material distribution inside the sensor; In soft-field tomography, the transmitting field does not follow the straight line pattern, and the signal distribution depends on the type of the excitation source. The nature of soft field is more complex−which makes image reconstruction relatively challenging compared with that of hard field [11]. Examples of soft-field tomography are Electrical Impedance Tomography (EIT), Electrical Capacitance Tomography (ECT), and Magnetic Induction Tomography (MIT), and these three are normally regarded as *"electrical tomography"*. The advantages of the electrical tomography are low cost and fast response.

Among the members of electrical tomography family, ECT is the most popular in industrial applications. It is a non-invasive and non-destructive imaging technique used in industrial process monitoring and evaluation. It consists of three main components: multi-electrode sensor, sensor electronics, and reconstruction and control (Figure 1).

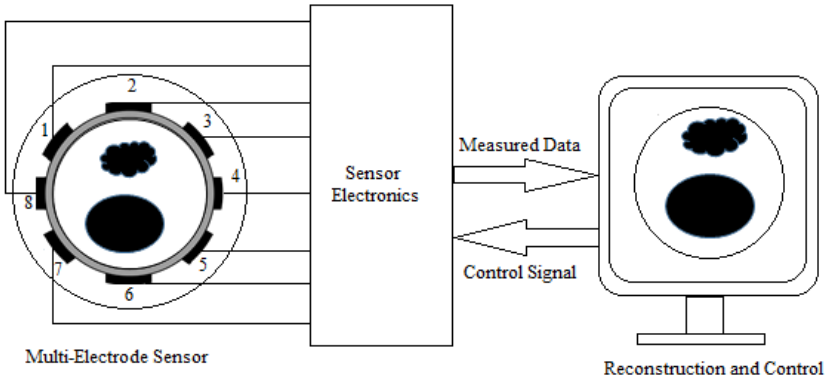

FIGURE 1. Typical ECT System

Multi-electrode sensor is an array of evenly spaced electrode arranged around the measuring object. Sensor electronics provides excitation signals and converts measured capacitances into voltages, which are then conditioned and digitized for data acquisition. Reconstruction and control implements image reconstruction algorithms and controls the system hardware. This paper reviews of image reconstruction methods used in ECT. The ECT system is first described, followed by revision of various image reconstruction methods.

2. Image reconstruction methods in ECT

2.1 ECT model representation

ECT image reconstruction involves solving two major computational problems: forward and inverse problems [20]. The forward problem calculates potential distribution from a known permittivity, and hence determines capacitance measurements. The inverse problem calculates permittivity distribution from the measured capacitance data. Results from the inverse problem are normally presented as a visual image, and hence the process is called image reconstruction. The relationship between capacitance and permittivity distribution is given by

$$C = -\frac{1}{V}\iint_{\tau} \varepsilon(x,y) \bigtriangledown \phi(x,y) d\tau, \tag{2.1}$$

where V is the potential difference between electrode pair forming capacitance, $\varepsilon(x,y)$ and $\phi(x,y)$ are respectively, permittivity and potential distribution, and τ is the electrode surface. In ECT image reconstruction, equation (2.1) is usually simplified as

$$C = SG, \tag{2.2}$$

where C is the normalized capacitance vector, S is the sensitivity matrix of normalized capacitance with respect to permittivity distribution , and G is a grey level vector. Equation (2.2) is called ECT model.

According to Yang et al. [40], there are three main challenges in ECT imaging: (1) the non linear relationship between the permittivity distribution and capacitance and the distortion of the electric field by the material present−the so called "soft-field" effect; (2) fewer number of independent measurements compared with pixels needed to reconstruct an image, and (3)

the inverse problem is ill−posed and ill−conditioned. The ECT solution is often sensitive to measurement errors and noise, and therefore unstable. To obtain meaningful reconstruction results, some prior information or constraints need to be added on the unknown variables.

Various numerical methods have been proposed to solve the ECT inverse problem. In general, they can be divided into two groups, direct and iterative methods [11, 22, 40]. Direct methods use a single mathematical step to calculate the permittivity distribution from the measured capacitance and the sensitivity matrix. Iterative methods optimize a set of objective functions iteratively until steady conditions are attained. A brief review of these methods is given in sections 2.2 and 2.3.

2.2 Direct reconstruction methods

2.2.1 Linear back projections

This method was the first to be used in ECT image reconstruction [37]. Using LBP, permittivity distribution is calculated from the liner mapping of measured capacitance and the sensitivity matrix as

$$G = S^T C, \tag{2.3}$$

where S^T represents the transpose of the sensitivity matrix, S. In LBP, the non-linear interaction (which is a function of permittivity value and distribution) between grey levels, is ignored. As a result, poor-quality images are generated that provides only qualitative information [40]. To obtain quantitative information, the use of other reconstruction methods or further processing is required.

2.2.2 Singular value decomposition

Singular value decomposition (SVD) is a matrix factorization method that has many applications, such as computation of the generalized inverse (pseudoinverse) of a non-square matrix [18]. In ECT imaging, sensitivity matrix, S, in equation (2.2) is an ill-posed (i.e. non-square), and can, therefore, be represented using SVD [39] as

$$S = U\Sigma V^T, \tag{2.4}$$

where columns of U are eigenvectors of SS^T, and columns of V are eigenvectors of S^TS, and Σ is a diagonal matrix of the same size as $S-$which is formed by the square roots of the nonzero eigenvalues of both SS^T and S^TS. Thus, the pseudoinverse, S^+, of S is obtained by

$$S^+ = V\Sigma^{-1}U^T, \tag{2.5}$$

and reconstruction equation becomes

$$G = S^+C. \tag{2.6}$$

SVD is considered as an effective method to solve inverse problems. However, the method reconstructs images with unsatisfying qualities.

2.2.3 Tikhonov regularization

Tikhonov Regularization (TR) is the most common method used in finding solutions for ill-posed problems [31]. In ECT, this method has been applied to solve the inverse problem [14]. Using TR, the inverse of the sensitivity matrix, S, is calculated by adding a regularization parameter. The mathematical details are summarized in equations (2.7) to (2.9). Equation (2.2) can be written in exact form as

$$S^TC = S^TSG. \tag{2.7}$$

From equation (2.7), G is calculated by

$$G = (S^TS)^{-1}S^TC. \tag{2.8}$$

In equation (2.8), S^TS is a non-invertible matrix, and a regularization parameter is thus introduced to form

$$G = (S^TS + \mu I)^{-1}S^TC, \tag{2.9}$$

where μ is a regularization parameter, and I is the identity matrix. The quality of reconstructed images strongly depends on the value of regularization parameter. A small value of μ gives a good approximation of permittivity distribution, but the solution highly affected by capacitance measurement error. Also, a large value of μ minimizes the capacitance measurement error, but increases the approximation error. To obtain grey levels close to true distribution, it is important

to choose an optimal regularization parameter. Currently, the choice of regularization parameter is done empirically in most ECT applications.

2.3 Iterative Reconstruction Methods

Iterative reconstruction methods are divided into two groups namely, algebraic reconstruction, and optimization methods [33].

2.3.1 Algebraic reconstruction methods

In algebraic reconstruction, image vector G, is estimated according to

$$G_{k+1} = G_k + \omega_k S^T (C - f(G_k)), \tag{2.10}$$

such that error between the calculated capacitance $f(G_k)$ and measured capacitance C is minimized, where G_k is the estimated image vector in the k^{th} iteration, $f(G_k)$ is the forward problem solution of image vector G_k, and ω_k is the gain factor of the k^{th} iteration$-$it gives distinct importance to specific parts of the measured capacitance vector.

Several algebraic reconstruction methods have been developed to solve the ECT inverse problem [11, 22, 40]. They differ into three aspects: (1) how the gain factor, ω_k, is applied, (2) how capacitance data are used to update the image vector, and (3) how pixels of the estimated image are updated. Some of these algorithms are explained in this section.

2.3.1.1 Iterative linear back projection (ILBP)

ILBP is an iterative generalization of LBP method (Section 2.2.1). The forward problem in ILBP is solved by using equation (2.2) and the gain factor, ω_k, is kept constant, and hence the image vector is updated according to

$$G_{k+1} = G_k + \omega_k S^T (C - SG_k). \tag{2.11}$$

ILBP uses only one set of measurement data in each iteration step, and therefore, generated images suffer from measurement data noise. The situation can be improved using simultaneous image reconstruction technique.

2.3.1.2 Simultaneous image reconstruction technique (SIRT)

In SIRT, all capacitance data are used to update the image vector at once [1]. The iterative formula for SIRT is given by

$$G_{k+1} = G_k - \omega_k S^T \frac{(SG_k - C)}{diag(SS^T)}, \tag{2.12}$$

where $diag(SS^T)$ is a vector composed of diagonal components of SS^T and the division means that each numerator is divided by the corresponding denominator. If necessary, ω_k can be replaced by a vector. This means that image vectors based on the number of equation (total number of measurements) are not treated equally when trying to obtain the average vector. This is important in improving the image quality in ECT as a non-linear system.

2.3.1.3 Iterative tikhonov reconstruction (ITR)

ITR is a generalization of standard Tikhonov regularization. In this method, image is updated according to

$$G_{k+1} = G_k + (S^T S + \mu I) S^T (C - SG_k). \tag{2.13}$$

Results generated by ITR method are better compared to many of the direct step methods. However this method is computationally inefficient and can only be used for off-line and research applications.

2.3.1.4 Landweber and Projected Landweber Iteration

Landweber iteration method is used to solve linear inverse problems [15]. In ECT, it has been used to solve inverse problem as given by Yang et al. [41] as

$$G_{k+1} = G_k - \alpha S^T (SG_k - C), \tag{2.14}$$

where α is a relaxation factor, and G_k is an initial image vector. Landweber is the fastest iterative method, but still requires many iterations to achieve steady conditions [13]. This makes Landweber algorithm unsuitable for imaging in on-line industrial processes. To reduce computational times, a preconditioner matrix proposed by Strand [28] can be applied, and the method

is called preconditioned Landweber [19] expressed as

$$G_{k+1} = G_k - \alpha D S^T (S G_k - C), \tag{2.15}$$

where D is a preconditioner matrix. For simplicity, D is normally chosen to be a diagonal matrix [3]. To ensure convergence at every iteration step, a projection operator P can be used to improve the overall convergence property of the Landweber iteration [40]. And the method is called Projected Landweber, expressed as

$$G_{k+1} = P\left[G_k - \alpha S^T (S G_k - C)\right], \tag{2.16}$$

P is defined by:

$$P[G_k] = \begin{cases} 0, & \text{if } G_k < 0 \\ G_k, & \text{if } 0 \leq G_k \leq 1 \\ 1, & \text{if } G_k > 1. \end{cases} \tag{2.17}$$

The projection operator ensures that the reconstructed images are non-negative and upper-bounded. The Landweber algorithm is computationally efficient compared with other iteration algorithms as it uses first order derivatives, but suffers from a semi-convergence condition [18] (image error decreases fast at the beginning of the iteration, but increases after reaching the local minimum point).

2.3.1.5 Model-Based Reconstruction

A model-based reconstruction (MOR) iterative method was proposed by Isaksen et. al [10]. In this method, the difference between measured and estimated capacitances is minimized by altering the dielectric constant distribution applied as the input to the sensor model. The process is repeated until the difference between simulated and measured capacitance is less than the pre-defined value. The iteration process of MOR algorithm is depicted in Figure 2.

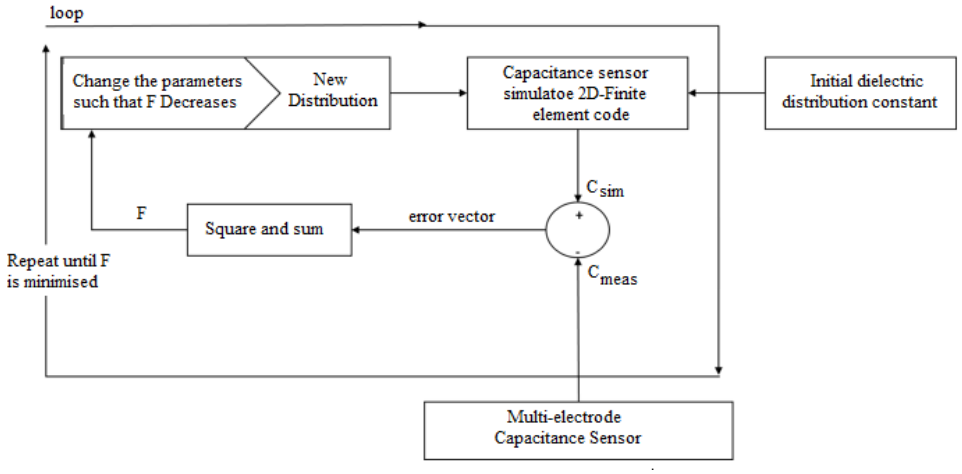

FIGURE 2. Model-based iterative reconstruction [10]

Studies suggest that MOR algorithm is more accurate with respect to both spatial resolution and components fraction estimation. However, the algorithm is slower [10, 24], and therefore recommended in off-line and research applications to determine optimal thresholding level to filter noise from LBP reconstructed image.

2.3.2 Optimization Reconstruction Methods

In mathematics, computer science, and operations research, mathematical optimization is the selection of a best element from some set of available alternatives[35]. In the simplest case, an optimization problem consists of maximizing or minimizing a real function by systematically choosing input values from within an allowed set and computing the value of the function. An optimization problem can be represented in the following way:

Given: a function $f : X \longrightarrow R$, from some set X to the real numbers. There is an element x_0 in X such that $f(x_0) \leq f(x)$ for all x in X ("minimization") or such that $f(x_0) \geq f(x)$ for all x in X ("maximization").

Such a formulation is called an optimization or a mathematical programming problem. Many real-world and theoretical problems may be modeled in this general framework. Typically, X is some subset of the euclidean space, R^n, often specified by a set of constraints, equalities or inequalities that the members of X have to satisfy. The domain X of f is called the search space or the choice set, while the elements of X are called candidate solutions or feasible solutions.

The function f is called, an objective function, a loss function or cost function (minimization), a utility function or fitness function (maximization), an energy function or energy functional [8]. A feasible solution that minimizes/maximizes the objective function is called an optimal solution.

Since image reconstruction in ECT is considered ill-posed and non-linear problem (i.e. there may exist more than one possible image as a solution for the reconstruction) optimization methods may achieve better results than other methods. Reported optimization methods that have been used in ECT include fuzzy mathematical Modeling [7], genetic algorithm [5], artificial neural networks [21, 22, 29, 33, 34], generalized vector sampled pattern matching method [30], total variation regularization method [4, 32], regularized total least squares [16], extended Tikhonov regularization [14], simulated annealing method [25], compressed sensing principle [36], population entropy and adaptive differential evolution [17], and least- squares support vector machine and a self-adaptive particle swarm optimization [6].

Studies suggest that optimization methods generate better image compared with algebraic reconstruction techniques [23, 34]. This is due to the ill-posedness nature of the in ECT inverse problem, which creates an additional challenge to the reconstruction problem when computational and experimental noise are present. Therefore, finding the solution based on minimization of the forward error function alone does not guarantee an optimum solution.

3 Experimental setup and evaluation criteria

3.1 Experimental setup

Experiments were carried out using an eight-electrode circular sensor ECT system. Eleven test distribution of annular and stratified flows were used. The tested methods include Linear back projection (LBP), Singular Value Decomposition (SVD), Tikhonov regularization (TKR), Iterative Tikhonov regularization (ITKR), Landweber iteration (LAND), and Projected Landweber iteration (PLAND). These methods were implemented using in MATLAB

3.2 Evaluation criteria

To evaluate the performance of implemented methods, both qualitative and quantitative metrics were used. Qualitatively, visual results of the reconstructed images generated by different methods were subjectively compared. To quantify the quality of results, the following quantitative metrics were used:

Relative Image Error (RIE): is the absolute difference between reconstructed and reference image vectors divide by the magnitude of the reference image vector [40], mathematically expressed as

$$\mathrm{RIE} = \frac{\parallel G^{rec} - G^{ref} \parallel}{\parallel G^{ref} \parallel}, \tag{3.1}$$

where G^{rec} and G^{ref} are, respectively, reconstructed and reference image vectors.

Distribution Error (DE): is an average of total sum of the absolute difference in grey level values between the reconstructed and reference image [10], expressed as

$$\mathrm{DE} = \frac{1}{n}\sum_{i=1}^{n}\left|G_i^{rec} - G_i^{ref}\right|, \tag{3.2}$$

where n is the total number of grey levels.

Correlation Coefficient (CC): between the reference image and the reconstructed image [38], calculated by

$$\mathrm{CC} = \frac{\sum_{i=1}^{n}(G_i^{rec} - \bar{G}^{rec})(G_i^{ref} - \bar{G}^{ref})}{\sqrt{\sum_{i=1}^{n}(G_i^{rec} - \bar{G}^{rec})^2 \sum_{i=1}^{n}(G_i^{ref} - \bar{G}^{ref})^2}}. \tag{3.3}$$

Gas Fraction Error(GFE): is the absolute difference between processed and reference gas fractions, expressed as

$$\mathrm{GFE} = \frac{\parallel \alpha^{rec} - \alpha^{ref} \parallel}{\alpha^{ref}}, \tag{3.4}$$

where α^{rec} andα^{ref} are, respectively, processed and reference gas fractions, and α^{rec} is calculated by

$$\alpha^{rec} = \frac{\sum_{i=1}^{n} A_i G_i^{rec}}{A_{pipe}}, \tag{3.5}$$

where A_i is the area of pixel element i, and A_{pipe} is the total area inside the pipe. Lower values of RIE, DE, GFE , and higher value CC indicate better performance.

4 Results and discussion

Figure 3 presents visual results from image generated using selected direct and iterative methods. From the results, we can clearly see that iterative methods, specifically, Projected Landweber, generate images with better qualities.

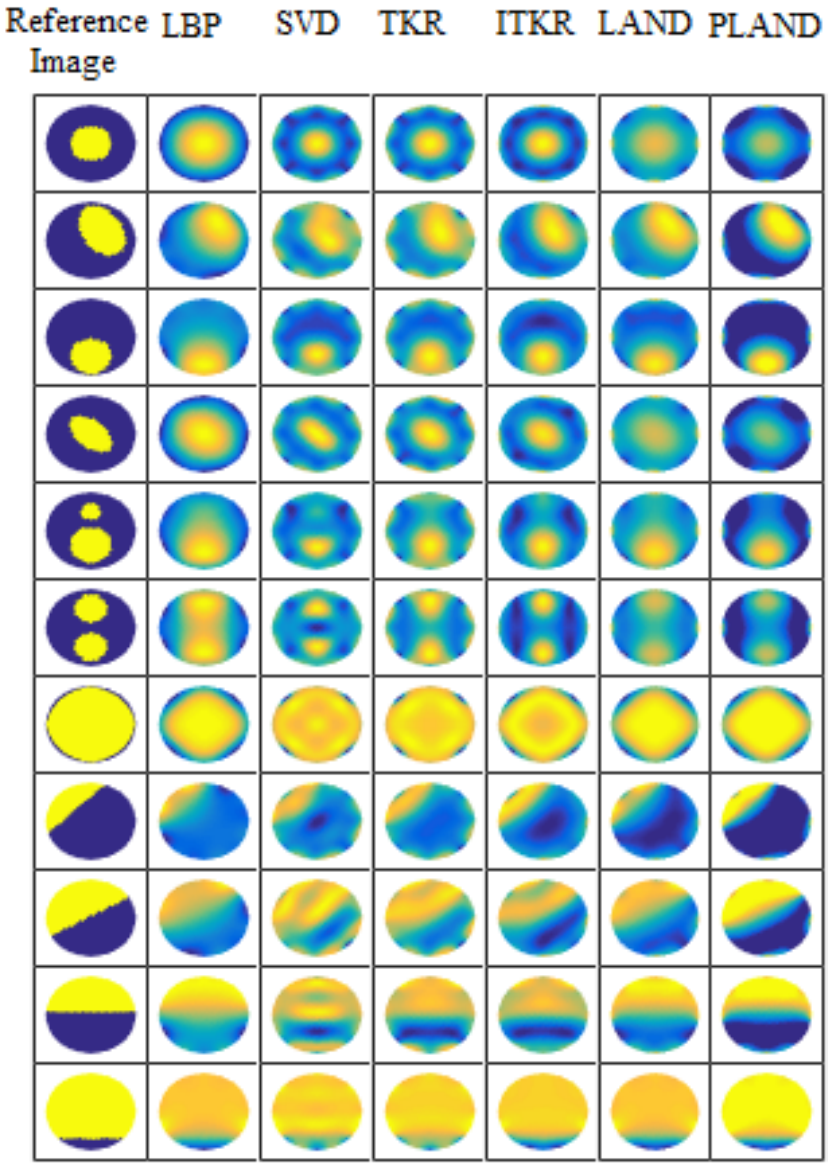

FIGURE 3. Images reconstructed from experimental data

Figure 4 shows quantitative results based on DE for each method over full component fraction range for annular flow. We noted that iterative methods are more accurate compared with direct methods over full component fraction range. However, the average DE for each method is

greater than 10%, suggesting that performance improvement is needed for these methods to be used for commercial application in oil industry.

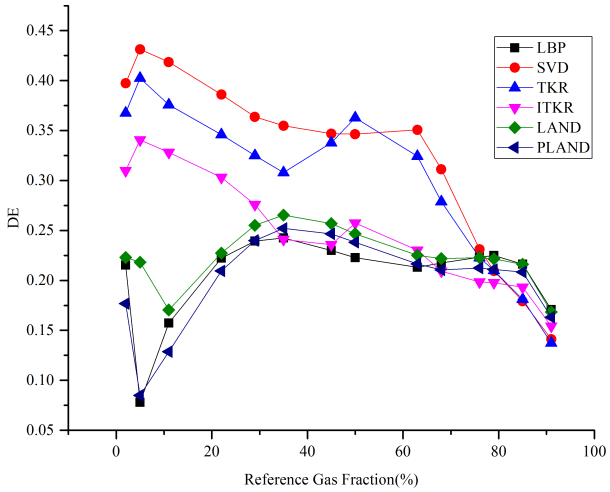

FIGURE 4. DE for annular flow over full component fraction range

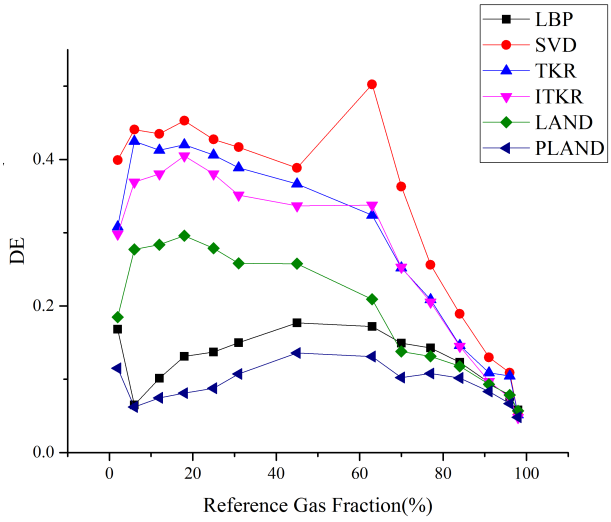

FIGURE 5. DE for stratified flow over full component fraction range

In Figure 5, performance DE results for each method for stratified flow over full component fraction range are presented. Again, we can see that results from iterative methods have minimum DE compared with direct methods. In particular, PLAND performs better over full component fraction range. However, the average DE for each method is greater than 10%, signaling the necessity of further improvement to actualize the methods in real life.

Performance results based on GFE for each method for dynamic on-line data over full component fraction range are presented in Figure 6. Results suggest that LBP performs slight better compared with other methods over full component fraction range. This is in contradiction with the results obtained using DE for annular and stratified flows.

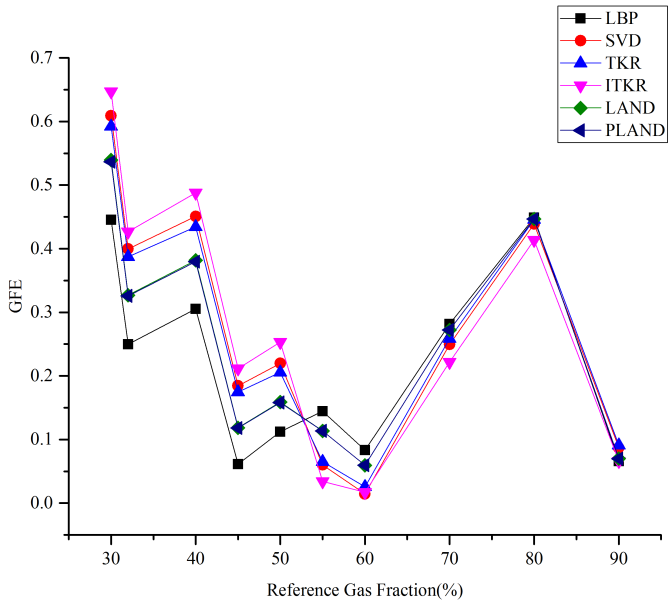

FIGURE 6. GFE for on-line dynamic data over full component fraction range

Table 1 presents quantitative results for selected annular and stratified flows based on RIE, DE, and CC. Time taken for each method to generate an image is also recorded in order to compare their reconstruction speeds. From results it is seen that iterative methods perform better than direct in terms of RIE, DE, and high CC.

TABLE 1. RIE, DE, CC and Time Elapse for selected annular and stratified flows

Algorithm	RIE (%)		DE (%)		CC		Time Elapse(Sec)
	Annular	Stratified	Annular	Stratified	Annular	Stratified	
LBP	43.35	32.67	31.87	17.47	0.595	0.885	0.597
SVD	57.28	41.15	34.84	50.27	0.36	0.041	0.858
TKR	42.89	37.05	30.44	14.98	0.738	0.848	1.33
ITKR	37.63	36.34	22.96	13.35	0.745	0.852	126.67
LAND	45.15	44.74	33.64	24.52	0.682	0.851	2.299
PLAND	38.05	30.94	24.18	12.14	0.745	0.895	1.98

Based on the above experimental analysis, iterative methods generate better images in terms of spatial resolution compared with direct methods. However, their computational time is greater than direct methods. This limit their usage for on-line industrial applications.

5 Conclusion

In this paper, a review of image reconstruction methods has been presented. Experimental results suggest that iterative methods generate better images compared with direct methods. However, they are computationally intensive. Also, most iterative methods are unstable and fail to generate globally unique solutions, and this calls for a need to establish more efficient and effective stopping mechanisms. However, achieving promising exit conditions in iterative methods has remained an open-ended research question.

ECT systems can fully be used in real-time applications, if both hardware and software are improved. In terms of hardware, work should focus on the design of sensors and sensor electronics circuits. On the sensing part, the focus should be on designing an optimal sensor structure including the number of electrodes. Selection of number of electrodes requires a trade-off between the numbers of measurements and unknowns (number of pixels or grey levels). Small number of electrodes will result in small number of measurements, and make the solution under-determined. Too many electrodes will give a small sensing area, this means very small capacitance will be measured accurately.

In terms of reconstruction methods, the design should focus on the application purpose of the ECT system, whether research investigation or real time industrial applications. For research investigations, relative slow but accurate methods can be implemented off-line. However, for monitoring and control of on-line industrial process, fast and accurate methods are needed. Therefore, the main focus of future work on reconstruction methods should be to design fast and accurate methods.

Conflict of Interests

The authors declare that there is no conflict of interests.

Acknowledgments

We are grateful to Nelson Mandela African Institution for funding this work and University of Dar es Salaam for allowing the us to use their ECT system for data collection and evaluation

REFERENCES

[1] BANGLIANG, S., YIHENG, Z., AND LIHUI, P. The use of simultaneous iterative reconstruction technique for electrical capacitance tomography. *Chemical Engineering Journal 77*, 1-2 (2000), 37–41.

[2] BECK, M., AND WILLIAMS, R. A. *Process tomography: principles, techniques and applications*, first edit ed. Butterworth-Heinemann, 1995.

[3] BENZI, M. Preconditioning techniques for large linear systems: a survey. *Journal of Computational Physics 182*, 2 (2002), 418–477.

[4] CHANDRASEKERA, T. C., LI, Y., DENNIS, J. S., AND HOLLAND, D. J. Total variation image reconstruction for electrical capacitance tomography. In *2012 IEEE International Conference on Imaging Systems and Techniques Proceedings* (July 2012), IEEE, pp. 584–589.

[5] CHANGHUA, M., LIHUI, P., DANYA, Y., AND DEYUN, X. Image reconstruction using a genetic algorithm for electrical capacitance tomography. *Tsinghua Science and Technology 10*, 5 (Oct. 2005), 587–592.

[6] CHEN, X., HU, H.-L., LIU, F., AND GAO, X. X. Image reconstruction for an electrical capacitance tomography system based on a least-squares support vector machine and a self-adaptive particle swarm optimization algorithm. *Measurement Science and Technology 22*, 10 (Oct. 2011), 104008.

[7] DEABES, W. A., ABDELRAHMAN, M. A., AND RAJAN, P. K. A fuzzy-based reconstruction algorithm for estimating metal fill profile in lost foam casting. In *2008 American Control Conference* (June 2008), IEEE, pp. 4868–4874.

[8] DIEWERT, W. E. Cost Functions. In *The New Palgrave Dictionary of Economics*, L. E. Durlauf, Steven N. and Blume, Ed. Palgrave Macmillan, 2008.

[9] HUA YAN, CHUNTING LIU, AND JING GAO. Electrical capacitance tomography image reconstruction based on singular value decomposition. In *Fifth World Congress on Intelligent Control and Automation (IEEE Cat. No.04EX788)* (2004), vol. 4, IEEE, pp. 3783–3786.

[10] ISAKSEN, O., AND NORDTVEDT, J. E. An implicit model based reconstruction algorithm for use with a capacitance tomography system. In *Proc. European Concerted Action on Process Tomography, Oporto* (1994), pp. 215–226.

[11] ISAKSEN, O. Y. A review of reconstruction techniques for capacitance tomography. *Measurement Science and Technology 7*, 3 (1996), 325–337.

[12] ITS. Applications of Process Tomography, 2014.

[13] JANG, J. D., LEE, S. H., KIM, K. Y., AND CHOI, B. Y. Modified iterative Landweber method in electrical capacitance tomography. *Measurement Science and Technology 17*, 7 (2006), 1909–1917.

[14] JING, L., LIU, S., ZHIHONG, L., AND MENG, S. An image reconstruction algorithm based on the extended Tikhonov regularization method for electrical capacitance tomography. *Measurement 42*, 3 (Apr. 2009), 368–376.

[15] LANDWEBER, L. An iteration formula for Fredholm integral equations of the first kind. *American Journal of Mathematics 73*, 3 (1951), 615–624.

[16] LEI, J., LIU, S., LI, Z., AND SUN, M. Image reconstruction algorithm based on the extended regularised total least squares method for electrical capacitance tomography. *IET Science, Measurement & Technology 2*, 5 (Sept. 2008), 326–336.

[17] LEI, S., JIANAN, L., AND YUMEI, Y. A Novel Image Reconstruction Algorithm based on Population Entropy and Adaptive Differential Evolution for Electrical Capacitance Tomography. *International Journal of Control and Automation 7*, 8 (2014), 303–310.

[18] LIU, C., AND CHANG, C. Novel methods for solving severely ill-posed linear equations system. *J. Marine Sci. Tech 17* (2009), 216–227.

[19] LU, G., PENG, L., ZHANG, B., AND LIAO, Y. Preconditioned Landweber iteration algorithm for electrical capacitance tomography. *Flow Measurement and Instrumentation 16*, 2-3 (2005), 163–167.

[20] MARASHDEH, Q., AND FAN, L. Electrical capacitance tomography-a perspective. *Industrial Engineering and Chemistry Research 47*, 10 (2008), 3708–3719.

[21] MARASHDEH, Q., AND WARSITO, W. Nonlinear forward problem solution for electrical capacitance tomography using feed-forward neural network. *Sensors Journal, IEEE 6*, 2 (2006), 441–449.

[22] MARASHDEH, Q., WARSITO, W., FAN, L.-S., AND TEIXEIRA, F. L. A nonlinear image reconstruction technique for ECT using a combined neural network approach. *Measurement Science and Technology 17*, 8 (Aug. 2006), 2097–2103.

[23] MARASHDEH, Q., WARSITO, W., FAN, L.-S., AND TEIXEIRA, F. L. A Multimodal Tomography System Based on ECT Sensors. *IEEE Sensors Journal 7*, 3 (Mar. 2007), 426–433.

[24] MWAMBELA, A., ISAKSEN, O., AND JOHANSEN, G. The use of entropic thresholding methods

in reconstruction of capacitance tomography data. *Chemical engineering science 52*, 13 (1997), 2149–2159.

[25] ORTIZ-ALEMÁN, C., AND MARTIN, R. Inversion of electrical capacitance tomography data by simulated annealing: Application to real two-phase gasoil flow imaging. *Flow Measurement and Instrumentation 16*, 2-3 (Apr. 2005), 157–162.

[26] PTL. Industries & Applications of Process Tomography, 2014.

[27] SOLEIMANI, M., WEI, H. Y., BANASIAK, R., YE, Z., YANG, C. L., QIU, W., YAO, A., MA, L., ADLER, A., AND PENGPEN, T. Volumetric soft field and hard field tomography: MIT, ECT, EIT, cone beam CT. In *7th World Congress in Industrial Process Tomography (WCIPT7)* (Krakow, 2013), University of Bath.

[28] STRAND, O. Theory and methods related to the singular-function expansion and Landweber's iteration for integral equations of the first kind. *SIAM Journal on Numerical Analysis 11*, 4 (1974), 798–825.

[29] SUN, T., MUDDE, R., AND SCHOUTEN, J. Image reconstruction of an electrical capacitance tomography system using an artificial neural network. In *1st World Congress on Industrial Process Tomography, Buxton, Greater Manchester, April 14-17, 1999* (1999), pp. 174–180.

[30] TAKEI, M., AND SAITO, Y. Application of the generalized vector sampled pattern matching method to reconstruction of electrical capacitance CT images. *Measurement Science and Technology 15*, 7 (July 2004), 1371–1381.

[31] TIKHONOV, A. Systems of differential equations containing small parameters in the derivatives. *Mathematical Sbornik 31*, 73 (1952), 575–586.

[32] WANG, H., TANG, L., AND CAO, Z. An image reconstruction algorithm based on total variation with adaptive mesh refinement for ECT. *Flow Measurement and Instrumentation 18*, 5-6 (2007), 262–267.

[33] WARSITO, W., AND FAN, L. network based multi-criterion optimization image reconstruction technique for imaging two-and three-phase flow systems using electrical capacitance tomography. *Measurement Science and Technology* (2001).

[34] WARSITO, W., AND FAN, L. Neural network multi-criteria optimization image reconstruction technique (NN-MOIRT) for linear and non-linear process tomography. *Chemical Engineering and Processing: Process Intensification 42*, 8-9 (2003), 663–674.

[35] WILLIAMS, H. *Model building in mathematical programming*. John Wiley & Sons, Inc., 2013.

[36] WU, X., HUANG, G., WANG, J., AND XU, C. Image reconstruction method of electrical capacitance tomography based on compressed sensing principle. *Measurement Science and Technology 24*, 7 (July 2013), 075401(7pp).

[37] XIE, C. G., HUANG, S. M., BECK, M. S., HOYLE, B. S., THORN, R., LENN, C., AND SNOWDEN, D. Electrical capacitance tomography for flow imaging: system model for development of image reconstruction algorithms and design of primary sensors. *IEE Proceedings G (Circuits, Devices and Systems) 139*, 1 (1992), 89–98.

[38] XIE, C. G., HUANG, S. M., LENN, C. P., STOTT, A. L., AND BECK, M. S. Experimental evaluation of capacitance tomographic flow imaging systems using physical models. In *Circuits, Devices and Systems, IEE Proceedings*- (1994), vol. 141, IET, pp. 357–368.

[39] YAN, H., LIU, Y., AND LIU, C. Identification of flow regimes using back-propagation networks trained on simulated data based on a capacitance tomography sensor. *Measurement Science and Technology* (2004).

[40] YANG, W. Q., AND PENG, L. Image reconstruction algorithms for electrical capacitance tomography. *Measurement Science and Technology 14*, 1 (2003), R1–R13.

[41] YANG, W. Q., SPINK, D. M., YORK, T. A., AND MCCANN, H. An image-reconstruction algorithm based on Landweber's iteration method for electrical-capacitance tomography. *Measurement Science and Technology 10*, 11 (1999), 1065 –1069.